Physical Properties of Polyphosphazenes. 2.† Poly[bis(trifluoroethoxy)phosphazene]

T. Masuko,‡ R. L. Simeone, J. H. Magill,*§ and D. J. Plazek

Metallurgical and Materials Engineering Department, University of Pittsburgh, Pittsburgh, Pennsylvania 15261. *Received July 26, 1983*

ABSTRACT: The behavior of poly[bis(trifluoroalkoxy)phosphazene] (PBFP) has been studied from 25 to 250 °C approximately by investigating the influence of temperature and cycle time upon creep compliance, volume change, spherulitic morphology, birefringence, and thermal properties. Unfractionated PBFP samples of high and low molecular weight were studied. The effect of aging upon properties, especially through the mesophase transition $T(1)$, were examined. Noticeable differences in mechanical behavior were observed depending upon the history or state of the sample. Hysteresis in the transition temperature determined by differential scanning calorimetry, creep compliance measurements, and dilatometry was observed. The curves of reduced densification and hardening due to aging measured dilatometrically and in creep, respectively, were superposable. Thus the decreases in volume and compliance appear to be mutually proportional to the degree of mesophase transformation from the 2D to the 3D crystalline state. This change can be described by a growth process with a B nucleation parameter of 680 K. This value is high compared to that observed in ordinary polymeric crystallization. Well-defined negatively birefringent spherulite films were obtained in solution-cast films. Melt-crystallized films usually contained needlelike aggregates of well-oriented crystals. Whenever PBFP specimens are heated through $T(1)$ the X-ray diffraction patterns degenerate to a single reflection, suggestive of a pseudohexagonal crystalline modification, which persists between $T(1)$ and T_m. The optical retardation measured within a single spherulite increases noticeably upon heating through this transition. However, afterward it remains invariant until the sample is heated to its true melting temperature when the birefringence finally reaches zero. Whenever the sample is melted, the spherulitic structure is lost.

Introduction

Polyphosphazenes have received much attention[1-10] since it was demonstrated[11] that stable linear macromolecules could be synthesized in a variety of chemical structures. During the past decade a large number of chemically different homopolymers and copolymers have been prepared and tested.[5,12-14] The physical properties of diverse materials have been studied, and measurements have been made by X-ray[15,16] and electron diffraction,[17] thermal degradation, including thermal analysis,[18,19] and differential scanning calorimetry[20] (DSC) for investigations of transitions. Dilute solution characterization[13,21] by viscometry, osmometry, light scattering, and gel permeation chromatography (GPC) has been made,[4] although difficulties have been encountered by several workers involving molecular association[22,23] in solution.

With the advent of solution polymerization[24,25] of cyclic halogenated oligomers, samples have been obtained that are usually of lower molecular weight and of narrower molecular weight distribution than the polymers prepared previously. These newer developments have prompted further interest in polymers with the chemical structure

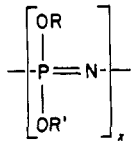

where R = R′ denotes a homopolymer and R ≠ R′ signifies a copolymer where R and R′ are randomly positioned along the chain backbone.

Surprisingly, these macromolecular polyphosphazene homopolymers exhibit mesophase behavior, even though they have considerable backbone flexibility akin to some polysiloxanes.[26] Conformational calculations[27,28] and infrared data[29] support the presence of significant chain backbone flexibility, but more study is required.

Sample preparation conditions affect the structure and properties[30] in the polymeric solid state of polyphosphazenes and marked effects are noted upon properties associated with the $T(1)$ transition. Annealing or heat treatment such as temperature cycling[31] through $T(1)$ increases the position and the magnitude of the enthalpy change of the transition. The X-ray diffraction spectrum is sharpened and specimen crystallinity is increased upon annealing and stretching homopolymeric specimens. Besides, dynamic properties[31] such as the loss tangent, δ, and the storage Young's moduli, E', are altered upon aging, and the role of enhanced crystallinity on these dynamic properties is manifested as decreasing values of tan δ and increases in the magnitude of E'. Recent rheological measurements[32] on aryloxy and alkoxy polyphosphazene copolymers (in solution) have been made. Investigations included steady-state and dynamic viscosities along with stress measurements.

Polyphosphazenes have useful biomedical[33,34] as well as technological applications.[13,35-37] Tensile,[13,31] flammability,[38] thermal stability,[39] and toxicity[40] properties have been studied, too, for a variety of polyphosphazenes. In view of the potential significance of polyphosphazenes in technological applications, it is appropriate to extend our knowledge and understanding into new research areas. Specifically, investigations of creep compliance, volume, and morphological characteristics are of fundamental importance in probing and understanding the molecular behavior of polyphosphazenes as a function of temperature and time. This paper represents a first in this direction.

PBFP was selected for more detailed study, since it exhibited two well-defined first-order transitions, i.e., a mesophase or $T(1)$ transition and another transition at the true T_m where an isotropic melt forms. Unique transition temperatures cannot be given because of hysteresis (see figures and discussion).

Experimental Section

Materials. The poly[bis(trifluoroethoxy)phosphazenes] (CA 28212-50-2) used in this study were kindly provided by Dr. G. Hagnauer of the U.S. Army Materials and Mechanics Research

† Presented in part at the 12th Annual NATAS Meeting, Sept 25–29, 1983, Williamsburg, VA. Reference 31 to be considered as part I in this series of papers.

‡ Present address: Yamagata University, Faculty of Engineering, Department of Polymer Chemistry, Jonan-4, Yonezawa-shi, Yamagata-ken, 992, Japan.

§ Also Chemical and Petroleum Engineering Department, University of Pittsburgh.

0024-9297/84/2217-2857$01.50/0

Table I
Molding Conditions for PBFP

sample[a]	disk dimens[b]	molding temp, °C	creep recovery[c]
1	1.77 × 5.13	250	53 (6), 52 (5)
2	9.40 × 3.13	180	

[a] Note that sample 1 was melted to an isotropic liquid before shaping and that sample 2 was molded in the mesophasic state between the $T(1)$ and T_m transitions. We refer to T_m as the true melting temperature where an isotropic melt is formed. [b] Height × diameter (mm × mm). [c] Number of runs is shown in parentheses.

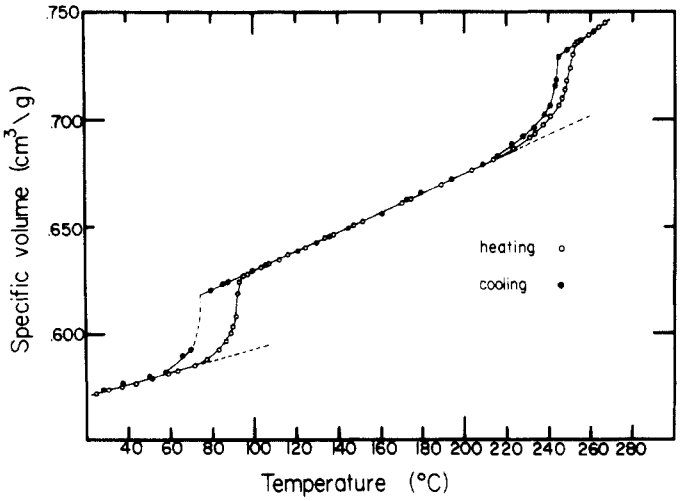

Figure 1. Specific volume vs. temperature plots for poly[bis-(trifluoroethoxy)phosphazene].

Center, Watertown, MA. The polymers had bimodal broad molecular weight distributions ($M_w/M_n > 10$) with weight-average molecular weights of 500 000 and 80 000, respectively. Both samples had acceptable elemental analysis, and they dissolved readily in tetrahydrofuran, indicating the absence of cross-linked material. Results reported have been obtained mostly on the higher molecular weight sample, but mention is also made of the lower molecular weight specimen studied elsewhere.[39]

Samples for creep measurements were molded into disks in two distinct ways in order to ascertain if fabrication history had an influence upon material behavior since mesophase formation was of considerable interest here. The molding conditions used for torsional creep specimens are documented in Table I. Sample 1 was a viscoelastic liquid that was shaped in situ and sample 2 was ductile and friable above T_1. The molding pressures were minimal, probably less than 1 kg/cm^2. The molding procedure is documented in ref 41.

PBFP was melted and outgassed in a vacuum system at 245 °C until it was free of bubbles, after which the dilatometers were filled with triply distilled mercury.

Films for optical and X-ray examination were case from tetrahydrofuran, and solvent was evaporated slowly to dryness. These spherulitic specimens were subsequently used for microscopic examination using a Mettler hot stage on a Leitz Ortholux microscope.

Methods. Dilatometry. PBFP samples of known mass, typically about 1.5 g, were sealed in cylindrical quartz bulb dilatometers fitted with a precision (1.5 mm) Pyrex capillary connected by quartz–Pyrex graded seals. Duplicate dilatometers were constructed to test for reproducibility. The dilatometer used for studying the overall transitional changes at $T(1)$ and T_m was not employed for kinetic and aging studies in the vicinity of $T(1)$ in order to minimize complications arising from thermal degradation. The dilatometer volume was read with a cathetometer using a fiducial mark on the capillary stem as a reference point. The precision was better than 0.001 cm^3/g. Controlled heating and cooling experiments were also carried out. Typical dilatometry data are shown in Figure 1.

Transformation kinetic runs were made dilatometrically by cooling the sample as rapidly as possible, 3 °C min^{-1}, in situ in the silicone oil bath, from the conditioning temperature (120 °C) to the isothermal temperature (see Figure 2).

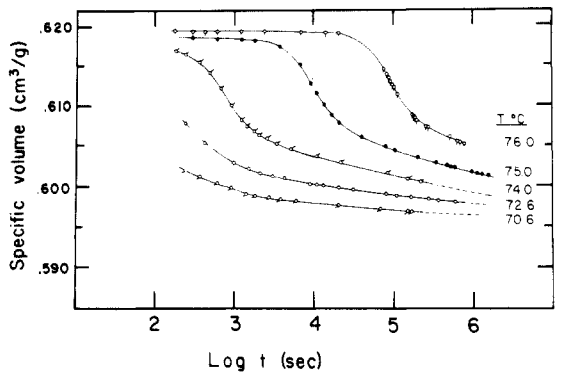

Figure 2. Volume contraction vs. aging time at several temperatures below the $T(1)$ transition. The PBFP sample was conditioned at 120 °C for 30 min before each run below $T(1)$.

We believe that the relatively slow cooling rate did not affect the isothermal densities much after the initial 100 s at the transformation temperature becuase of the small temperature range involved in the contraction measurements. For instance, at 77 °C, no measurable contraction occurred in the dilatometer in 24 h. Even at 75 °C, the induction period for the phase change was about an hour. Therefore, there can be no question that a cooling rate of 3 °C min^{-1} influenced results at 75 °C or above. To reach 74 °C from 75 °C took about 20 s. Aging times were measured from the moment the bath temperature reached the selected transformation temperature. Due to relatively low thermal conduction, a temperature lag in the polymer sample during the cooling caused an unaccounted for delay which must yield specific volumes that were too high at short aging times, while, simultaneously, the relatively slow cooling rate yielded premature sample contraction. These two presumed errors tend to offset each other. To cool the dilatometer contents from 75.0 to 70.6 °C took about 10^2 s so that the readings of the specific volume taken at short times (between 10^2 and 10^3 s) could be in error so that the temperature shift factor obtained for the 70.6 °C temperature measurement would also be affected. Other measurements made on the lower molecular weight PBFP by switching the dilatometer rapidly between baths of different temperatures (conditioning and transformation) have yielded similarly shaped curves which appear to be reducible as do those presented in this paper. Absolute results are not yet available since the dilatometer has not been calibrated because other measurements are in progress. The even slower equilibration of the creep instrument housing and sample is accounted for by disregarding data taken before about 10^4 s of aging time. In the dilatometer runs (Figure 2) precautions were also taken to exclude suspect data points.

Creep Measurements. Torsional creep measurements were made by using a magnetic-bearing torsional creep apparatus (MBTCA) already described in detail in the literature.[42] Compression-molded specimens shaped into right circular cylinders were a translucent light tan color. Since sample 2, which was never heated above T_m, proved to be slippery and friable above $T(1)$, it was cemented between the platens of the MBTCA instrument with epoxy resin at room temperature where it was like a hard wax. We are confident that diffusion of the epoxy into the PBFP was negligible. In any case the level, but not the shape, of our $J(t)$ curves would be affected slightly by a rigid sample surface layer. Sample 1 self-adhered to the instrument platens after it was melted above T_m, when it was shaped in place and subsequently cooled. We have never encountered a molten polymer with viscosities less than 10^7 P that did not wet and adhere to clean metal surfaces.

Creep runs were conducted at constant temperature under a 10–15 μmHg vacuum. Measurements were made on sample 1 in the temperature range 76–182 °C. The creep compliance results as log $J(t)$ are plotted vs. log t in Figure 3. For sample 2 (unmelted, i.e., fabricated < T_m), two heating series were employed sequentially: (i) from 24 to 110 °C (see Figure 4) and then (ii) from 26 to 156 °C (illustrated in Figure 5). The sample form coefficient was obtained by using in situ height measurements

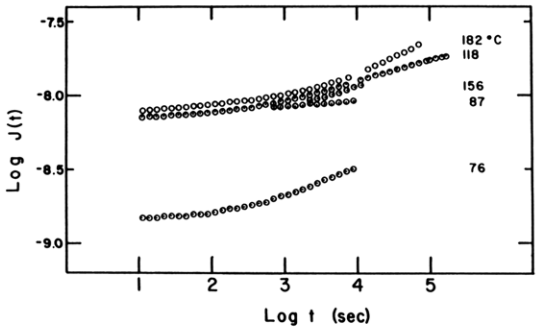

Figure 3. log (creep compliance) (cm^2/dyn) vs. log t (s) for sample 1 (melt crystallized). Data points for runs at 87 and 156 °C coinciding points are omitted for clarity. The order of runs was 118, 156, 182, 87, and 76 °C.

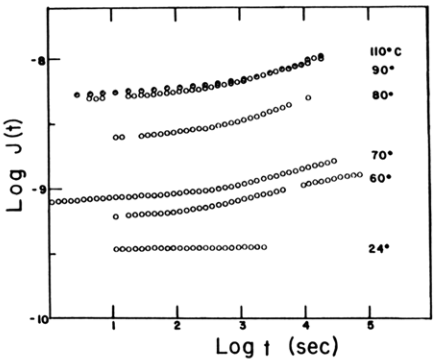

Figure 4. log (creep compliance) (cm^2/dyn) vs. log t (s) for sample 2; first heating cycle.

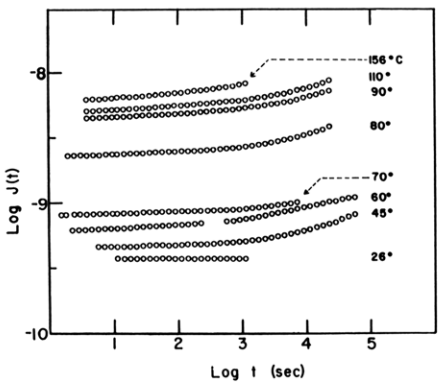

Figure 5. log (creep compliance) [log $J(t)$] (cm^2/dyn) vs. log t (s) for sample 2; second heating cycle.

made at temperature and the corresponding density data, from dilatometry, as shown in Figure 1.

Optical Microscopy. Spherulites in film form obtained by solution casting from THF were characterized between polaroids using a 6-order Berek compensator. Figure 6 shows typical negatively birefringent spherulites crystallized from THF solution. Figure 7 illustrates the measured optical retardation of such a spherulite as a function of heating and cooling, expressed as $\langle \Delta n \rangle \bar{t}$, where the birefringence is $\langle \Delta n \rangle$ and the average specimen thickness is $\bar{t}$.

X-ray Diffraction. The molecular orientation within a solution-cast PBFP spherulite was also determined by X-ray diffraction using a 30-μm-diameter X-ray beam in a Philips vacuum camera. Cu Kα radiation was used. A typical microbeam X-ray diffraction pattern insert of a negatively birefringent spherulite is shown in Figure 6. In parts a and b of Figure 8, Debye–Scherrer diffraction patterns obtained at room temperature (25 °C) and at 120 °C (above $T(1) \sim 85$ °C), respectively, are shown. A structural change is evident on passing through $T(1)$, as reported[13,16] in the literature.

DSC Measurements. These measurements were made with a Perkin-Elmer DSC-2 calorimeter fitted with data-processing accessories. Two types of experiments were carried out. One employed a fixed heating rate. An example is shown in Figure

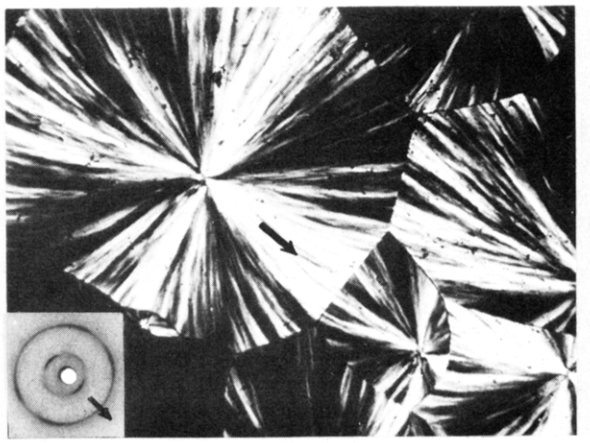

Figure 6. Negatively birefringent spherulites grown from THF solution at room temperature. The microbeam X-ray diffraction pattern of these spherulites in the insert was taken with Cu Kα radiation using a 30-μm collimator. Arrows indicate spherulite radius directions.

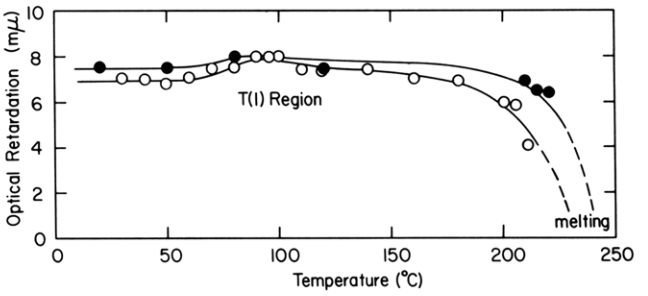

Figure 7. Optical retardation measurements on individual spherulites of PBFP (formed from THF solution) as a function of cycling temperature through the $T(1)$ region: (○) heating; (●) cooling/reheating.

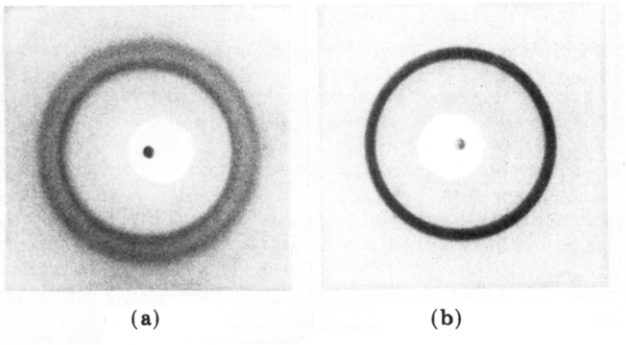

Figure 8. Diffraction pattern from unoriented PBFP spherulite sample using Cu Kα radiation at (a) room temperature and (b) 120 °C (i.e., above the $T(1)$ transition).

Table II
Effect of Fabrication Conditions on $\Delta H[T(1)]$ for a 10 °C min^{-1} Heating Rate

sample	$\Delta H[T(1)]$,[a] cal g^{-1}	$T(1)$ peak, K
solution cast from THF	7.36	355.5
5° °C min^{-1} cooling[b]	6.86	361.5
10° °C min^{-1} cooling[b]	6.66	358.8
20° °C min^{-1} cooling[b]	6.47	357.3
40° °C min^{-1} cooling[b]	6.43	356.9
80° °C min^{-1} cooling[b]	6.16	356.8
liquid N_2 quench	5.99	354.0

[a] Highest value attained by us through annealing and/or temperature cycling was 8.7 cal g^{-1}. [b] All cooling rates were made from 393° to 300 °K.

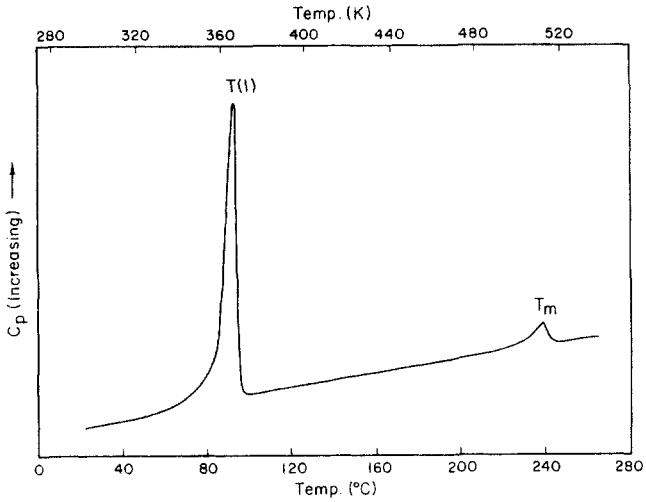

Figure 9. DSC curve of poly[bis(trifluoroethoxy)phosphazene] showing two first-order transitions at $T(1)$ and T_m, respectively, after the polymer was crystallized from the melt.

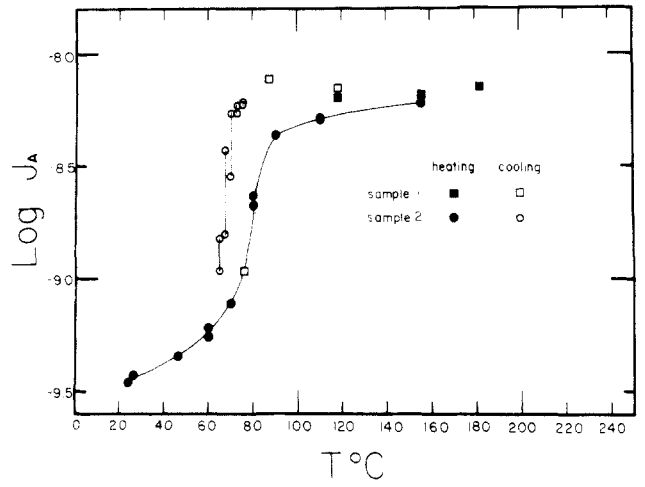

Figure 10. log (creep compliance), (J_A) (cm^2/dyn) vs. temperature (°C) for heating and cooling of samples 1 and 2.

9. In the other type, fixed heating and variable cooling rates were used. The results are tabulated (see Table II). In addition, the polymer sample was cycled 30 times through the $T(1)$ region at controlled heating and cooling rates to determine the effect of aging on specimen stability manifested via changes in its enthalpy and "melting" profile.

Results and Discussion

This investigation was concerned with studying the volume and compliance behavior near the $T(1)$ transition in PBFP since no measurements of this kind have appeared in the literature. Other techniques such as DSC, X-ray, and optical measurements were also made in the vicinity of the $T(1)$ transition. Some volumetric and other measurements were also made at the much higher melting temperature T_m, where some degree of depolymerization has been reported.[11] Because of anticipated problems here, we focused our attention primarily upon the $T(1)$ region.

$T(1)$ Transition. The $T(1)$ phase change is clearly manifested by a 0.7-decade increase in log $J(t)$ in the interval 70–90 °C from creep measurements. (See Figures 3–5 and 10.) A comparable change in magnitude was reported recently[31] in storage modulus, E', upon traversing a similar temperature span using another PBFP sample. From dilatometry (Figure 1) a 6.1% volume change occurs upon traversing this $T(1)$ interval. The $T(1)$ transition cited here does not have a unique value, but its position on the temperature scale depends upon sample history (see Figure 1 and Table II). The magnitude of the enthalpy change in DSC also indicates a relatively high crystallinity since $\Delta H_f[T(1)]$ is 7.4 cal g^{-1}. The highest value reported[16] for PBFP is $\Delta H_f[T(1)] = 8.7$ cal g^{-1}, which agrees favorably with our highest value, too. Changes in sample volume and in the log of an "instantaneous" compliance, J_A, occur with time of aging along isothermal lines (Figure 10). The J_A values were obtained graphically (Figure 11) as intercepts on the ordinate axis of $J(t)$ vs. $t^{1/3}$ plots (i.e., as Andrade creep plots,[42] where $J(t) = J_A + \beta t^{1/3}$. Although all of these lines are not strictly linear, the uncertainties in J_A were minimized since values were derived only from the slopes of the shorter time portions of these Andrade plots. β is a characterizing constant. Likewise in DSC runs, a noticeable shift in the position and the magnitude of the enthalpic heat of the transition were noted and reported elsewhere,[5,16] too. Cooling rates (Table II) significantly alter the enthalpy.

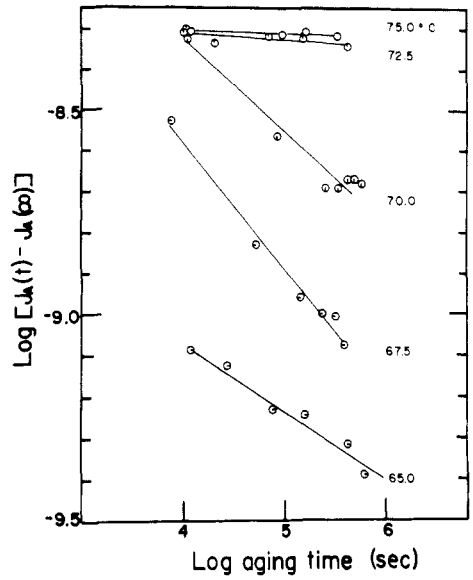

Figure 11. Logarithm of the difference of $J_A(t')$ on cooling and $J_A(\infty)$ on heating vs. log (aging time) (s). Points are shown in Figure 4 as sample 2 cooling.

In all aging creep runs the sample was preconditioned initially at 110 °C. Sample 2 prepared as described in Table I was tested by cooling it to room temperature followed by heating to 156 °C in order to equilibrate it in the mesophase state before cooling again. Results in Figure 5 show that the log $J(t)$ vs. log t curves appear to be shifted to longer times relative to the first heat treatment (Figure 4). The slopes, expressed as d[log $J(t)$]/d[log t], are observed to be lower at corresponding temperatures and times. Slightly higher compliance curves, corresponding to a lower degree of crystallinity, are observed for the melt-crystallized material (Figure 3) compared with the material that was never melted (see Figures 4 and 5). Two creep runs performed at 118 °C on sample 1 before and after prolonged holding (48 h at 156 °C) show that the compliance[53] increased slightly (within experimental uncertainty, <5%). If this change is indeed attributable to a decrease in molecular weight, its effect was never noticed during dilatometric measurements (see Figure 1) along the equilibrium volume line above $T(1)$, where the experimental error if <0.2%. Even so, the magnitude of the anticipated discrepancy may lie within this range.

Time–Temperature Superposition. (1) Creep Measurements. Since the curves of Figures 3–5 do not show a significant change in slope with temperature, superposition plots were not made for the limited creep data

available. It was estimated that more than 10^6 s would be required to reach a long-time asymptote, if indeed one exists. Such persistent long-time creep[43] is characteristic of crystalline polymers.

(2) Volume Contraction. The volume–time plots of Figure 2 are superposable. It must be realized that PBFP still has an appreciable amorphous content even below $T(1)$ because it exhibits a measurable glassy transition at −66 °C, approximately.[16,31] Still, the volume contraction curves indicate that the mechanism of transformation is the same at all measured temperatures (see Figure 2). Therefore, the nucleation/growth mechanism from the thermotropic (2D) state to the more ordered (3D) state is independent of the transformation temperature. This appears true because the reduced contraction curves do not change shape with temperature. Inspection of Figures 1, 2, and 11 supports the notion that the onset of the phase change (2D → 3D) is not complicated by the slow cooling rates used. Clearly, cooling from 120 to 74 °C occurs without a measurable phase change.

Besides these observations it is worth recording parametric data on the volume–temperature expansion of PBFP (Figure 1) below and above $T(1)$ and in the amorphous melt above T_m. These values are as follows: below $T(1)$ (25–52 °C), $\alpha_c = 2.48 \times 10^{-4}$ (K^{-1}); above $T(1)$ (97–175 °C), $\alpha_{T(1)} = 6.99 \times 10^{-4}$ (K^{-1}); above T_m (254–267 °C), $\alpha_l = 9.24 \times 10^{-4}$ (K^{-1}). Here, $\alpha_i = (1/V)(\partial V/\partial T)_P$ is the appropriate expansion coefficient. From X-ray measurements[43] a value of $\alpha_{T(1)}$ of 1.74×10^{-4} for the "a"-axis direction between 100 and 200 °C for solution-cast film has been obtained, compared with a literature value[45] of expansion of 1.8×10^{-4} (K^{-1}). For melt-cast film (in the same range) we obtained 2.7×10^{-4} for $\alpha_{T(1)}$. A wide melting range is noted by dilatometry starting at 210 °C and reaching the liquidus at 253 °C. Upon cooling the PBFP melt in the dilatometer, we observed hysteresis, but it is not as extensive as that found on passing through the $T(1)$ region. This dilatometric melting span is even broader in the lower molecular weight PBFP sample. Crystallization experiments made on samples between glass coverslips using an optical hot stage microscope also indicate that extensive undercooling is not possible before the onset of mesophase formation occurs approximately 10 °C below T_m.

Aging Studies. Creep experiments were time-consuming experimentally since our sample temperature could not be changed rapidly owing to the thermal inertia of the equipment, and only data taken after 3 h of aging time could be trusted.

Still, a series of useful creep runs were performed on sample 2 after it had been cooled from the conditioning temperature, 110 °C, to lower temperatures within the $T(1)$ transformation region. Creep compliance measurements were made repeatedly after reaching each temperature in order to evaluate the effects of isothermal contraction on the creep compliance behavior. Dilatometry runs have already indicated that significant volume changes occurred below $T(1)$ (see Figure 2). Aging creep runs, except those carried out at 70 °C, were always preceded by heating the polymer to 110 °C, thus allowing the sample time to equilibrate above the $T(1)$ transition, before cooling it down again. (Note an exception to this procedure, however, where the same was held at 90 °C prior to aging at 70 °C.) The specific volume data in Figure 1 and DSC results (Figure 9) both indicate that the $T(1)$ transition only occurs well below 110 °C for the higher molecular weight specimen reported in this creep work.

Spherulite Morphology. Crystallization of PBFP from THF solution always yields negatively birefringent spherulites as seen in Figure 6. These spherulites exhibit a relatively well-defined Maltese extinction cross when viewed between crossed polaroids. The molecular chain orientation is predominantly perpendicular to the radius[44] of the spherulite, with the crystallographic "a" direction of the unit cell lying along the radial direction (see microbeam X-ray diffraction insert). There is some angular spread or dispersion of the crystallite orientation about the growth direction as indicated by the length of the diffraction arcs. However, some of this dispersion stems from the divergence of the lamellae within the 30-μm X-ray beam itself, compared to the radius of the spherulite (200 μm approximately), in Figure 6. Still, the crystallite orientation is relatively well-defined within these spherulities.

The optical retardation of single spherulites measured by a Berek compensator using green light increases measurably upon heating corresponding to the first run (open circles). Upon subsequent cooling (filled circles) and/or further heating/cooling, the birefringence is essentially invariant with temperature through $T(1)$. The birefringent changes at $T(1)$ are less apparent than the 6% volume change by dilatometry (see Figure 1) and the large transition enthalpy[5,20,31] from DSC measurements. DSC and dilatometric measurements provide average or nondirectional properties of the polymer whereas the birefringence change is representative of the mean orientational change within a 200-μm-diameter spherulite. Structurally, the unit cell goes from orthorhombic below $T(1)$ to pseudohexagonal above it with no measurable alteration in the "a" direction of either structure (evidence from electron/diffraction in thin films (Kojima and Magill,[44] unpublished)).

A change in the transmitted light intensity obtained from a spherulitic PBFP film has been reported[45] on heating through the $T(1)$ region. This change from a 3D to a configurationally disordered thermotropic phase and/or vice versa seems to be in accord with a large entropic change[46] induced by side-group disorder. The descriptor "condis" has been introduced recently to distinguish the thermotropic crystal from a plastic crystal[47] such as tricyclodecane, or the conventional organic liquie crystal[48] that is usually employed to describe small molecules that exhibit mobile mesophases. In the PBFP materials local mobility in the mesophase is relatively high based upon creep measurements obtained on melted and unmelted polymer molded according to the conditions in Table I. Upon traversing $T(1)$, side-group librations induce considerable conformational disorder as manifested via DSC (see, for example, Figure 9), X-ray (Figure 8), and electron diffraction[30] and also the onset of molecular mobility witnessed in the broad-line NMR spectrum for the same type of polymer.[49] (The transition from an orthorhombic to a pseudohexagonal structural modification shows that "a"-axis orientation is maintained throughout (Kojima and Magill, to be published.[50])

Polyphosphazene Mesophases. At present one of the most meaningful classifications of liquid crystalline phases is due to Wunderlich and Grebowicz[46] since liquids flow[54] and creep experiments on PBFP show no evidence of viscous flow below T_m. Low intrinsic conformational barriers to rotation in polyphosphazenes comply with the flexible-chain backbone nature of these macromolecules. *Molecular stiffness is not necessarily a criterion for it in mesophase formation even though it may be a sufficient condition for inflexible rodlike molecules.* Note however that the expansion coefficient in the $T(1)$ regime is about intermediate between the crystalline, α_c, and the melt, α_l, parameters. Dilatometric thermal analysis, creep, and

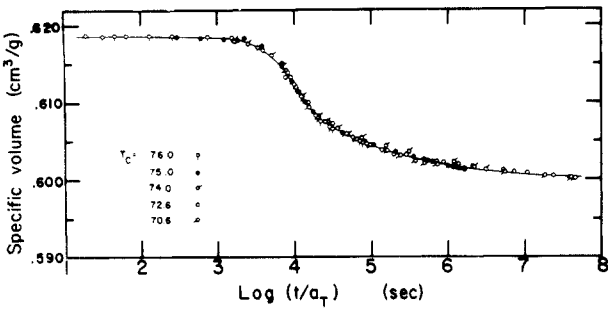

Figure 12. Superposition of dilatometric volume transformation curves (Figure 2) depicting rates corresponding to in situ cooling below the $T(1)$ transition. T_c = 75 °C was used as a reference state, T_r, for the data reduction.

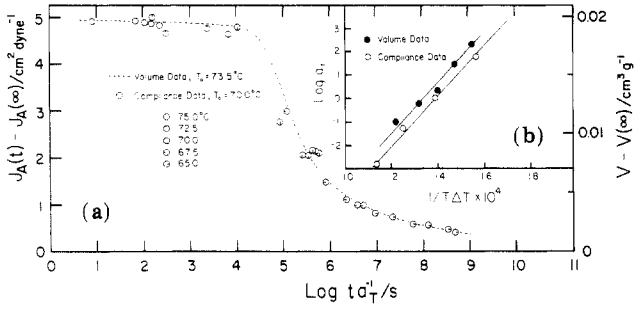

Figure 13. (a) Specific volume and "instantaneous" compliance deviations from equilibrium at reduction temperatures of 73.5 and 70.0 °C, respectively, shown as a function of the logarithm of reduced aging time [log (t/a_T)]. The poly[bis(trifluoroethoxy)phosphazene] creep sample was never melted, whereas the dilatometric specimen was melted at 245 °C. (b) Logarithm of the temperature shift factor, $a_T = R(T_0)/R(T)$, where R is the transformation rate at the chosen reference temperature T_0 and at the measurement temperature T, respectively, given as a function of $(T\Delta T)^{-1}$. Filled points from volume data shown in Figure 2 and open circles from "instantaneous" compliances J_A shown in Figure 11.

dynamical mechanical (Rheovibron) measurements all indicate that there is a very strong dependence of molecular properties upon thermal history. Noteworthy is the structural change (or changes) manifested by both X-ray (Figure 8) and electron diffraction[50] and the onset of side-chain mobility by broad-line NMR.[49]

From a thermodynamic viewpoint the conformational disorder in PBFP may be quantified to a degree through the ratio of the magnitude of the enthalpy change at $T(1)$ compared to the value at T_m, $\Delta H[T(1)]/\Delta H[T_m]$, typically about 10/1. The change in the degree of disorder may be expressed as an entropy ratio, $\Delta S[T(1)]/\Delta S[T_m]$, estimated to have a value of 1. Considerably higher values have been quoted for a (aryloxy)phosphazenes,[46] where thermal degradation is often encountered at the more elevated temperatures required to melt these systems. Even so, the extensive ordering ↔ disordering that occurs upon cooling and heating through the $T(1)$ region is significant and seems to be in line with the relatively large volume change encountered at $T(1)$ for PBFP.

Complete disordering in PBFP (i.e., the formation of an isotropic melt) occurs whenever the polymer undergoes a *further* 5.9% volume change at T_m even though the enthalpy change is small. Overall these two transformations, seemingly first order, however measured, are substantial and also significant from a mechanical properties viewpoint.

Transformation Kinetics below the $T(1)$ Transition. Surprising consistency is noted in the reduced time–temperature plots in Figures 12 and 13, suggesting that similar molecular processes are contributory to both of these property changes even though the particular dilatometer sample alluded to was initially melted, whereas the material (sample 2) used in the creep measurements was never heated about 180 °C.

It is noteworthy that all the volume transformation rates can be reduced to a single curve for the $T(1)$ crystallization. This process apparently involves a two-dimensional nucleation mechanism expressed[51] as

$$\ln (R\zeta) = \ln R_0 - BT(1)/T\Delta T \qquad (1)$$

where R is the transformation rate and ζ is the local friction factor (assumed to be temperature independent within the 10 °C interval of the measurements in this paper). R_0 is a constant and the undercooling $\Delta T = (T(1) - T)$, which corresponds to the difference between the first-order equilibrium $T(1)$ temperature and the transformation or crystallization temperature in question (see Figure 2). B is a parameter associated with crystal surface energies and may be expressed as

$$B = 4\sigma_e\sigma T(1)/\Delta h(1)k \qquad (2)$$

Here, σ and σ_e are the lateral and surface (or interfacial) energies of the crystal respectively, $\Delta h(1)$ is the true enthalpy of the transition, and k is Boltzmann's constant.

The "instantaneous" compliance values (Figure 11) obtained during aging are shown in Figure 13a. A reference temperature of T_0 = 70 °C was used compared with a value of 73.5 °C for volume data from Figure 12. (Note that the different T_0 values arise because of the different sample histories outlined earlier in the text; e.g., see Table I). The volume and compliance plots (see Figure 13b) when expressed as a function of $(T\Delta T)^{-1}$ (see eq 1) each give rise to identical values of B = 680 ± 10 K obtained from the slopes of these linear plots. Once again the $T(1)$ reference state values employed in the analysis were in keeping with sample histories. Specifically $T(1)$[unmelted] = 91 °C and $T(1)$[melt crystallized] = 94.5 °C, which are in reasonable agreement with DSC and dilatometric measurements. Thus, the melting shifts both the transition temperature and the aging response by 3.5 °C. The V_∞ was estimated from Figure 12 to be 0.599 cm³/g, and from Figure 10, $J_A(\infty)$ values were obtained from the heating curves only. The calculated B value is much higher than that for any conventional amorphous–crystalline transformation, which is a less ordered starting point than for the mesophase 2D-to-3D transformation. For most polymers, B parameters lie below 350 K in most cases. Either the anisotropy of the $T(1)$ transition cannot be accounted for within the crystallization framework used in eq 2 or a considerably rough surface interface may arise in transforming from the domain structure of the thermotropic to the 3D crystalline state. Evidence favoring the latter position is too scant presently for a stronger statement at this time.

Since annealing of PBFP via temperature cycling in the DSC causes an increase in the position of $T(1)$ and in the magnitude of the enthalpy of this transition,[16,31] this process allows the polymer to become better ordered whenever the specimen is cooled again.[50] (The heat of the $T(1)$ transformation (see Table II) decreases linearly with log (cooling rate) in the range 5–80 °C min⁻¹.) With temperature cycling, the melting peak, T_m, noticeably broadens and decreases slightly in value,[31] too, as the state of the specimen changes. Likewise, cycling the PBFP specimens (in dilatometeric experiments) repeatedly through T_m results in a noticeable lowering of the melting temperature, in accord with the DSC observations.

From the literature,[16,31] it appears that the two transitions encountered in PBFP are more evident than in most

other higher melting polyphosphazenes, some of which undergo substantial degradation[20] when they are heated close to their melting points.

Whenever cycling studies are restricted in PBFP to temperatures well below T_m, the degree of depolymerization,[11] if it occurs, appears to be insignificant. Dilatometry, creep, birefringence, and most DSC measurements were restricted to temperature regimes where only changes in sample order occurred well below T_m. Improved molecular packing in line with a more precise description of these changes is essential in practical applications of PBFF as an engineering material. Decreasing creep rate, higher density, and lower loss tangent values[31] (and increasing moduli) have been found for this polyphosphazene as a consequence of thermal cycling.

Acknowledgment. We are indebted to Drs. Robert Singler and Gary Hagnauer of the Army Materials and Mechanics Center, Watertown, MA, for the polyphosphazene samples. Thanks for partial support of the project is expressed to the National Science Foundation, Polymers Program of the Materials Division (J.H.M.), and the Chemical and Biological Processes Program of the Engineering Division (D.J.P.) under Grants DMR 8113089 and CPE-8024713.

References and Notes

(1) H. N. Stokes, *Am. Chem. J.*, **19**, 782 (1897).
(2) J. E. Thompson and K. A. Reynard, *J. Appl. Polym. Sci.*, **21**, 2575 (1977).
(3) H. R. Allcock, *Angew. Chem., Int. Ed. Engl.*, **16**, 147 (1977).
(4) G. L. Hagnauer and N. S. Schneider, *J. Polym. Sci., Part A-2*, **10**, 669 (1972).
(5) R. E. Singler, N. S. Schneider, and G. L. Hagnauer, *Poly. Eng. Sci.*, **15**, 34 (1975).
(6) H. R. Allcock, G. Y. Moore, and W. J. Cook, *Macromolecules*, **7**, 571 (1974).
(7) H. R. Allcock, *Makromol. Chem., Suppl.*, **4**, 3 (1981).
(8) G. L. Hagnauer and B. R. Laliberte, *J. Appl. Polym. Sci.*, **20**, 3073 (1976).
(9) T. C. Cheng, V. D. Mochel, H. E. Adams, and T. F. Longo, *Macromolecules*, **13**, 158 (1980).
(10) V. V. Korsak, S. V. Vinogradov, D. R. Tur, N. N. Kasarova, L. I. Komarova, and L. M. Gilman, *Acta Polym.*, **30**, 245 (1979).
(11) H. R. Allcock, R. L. Kugel, and K. J. Valan, *Inorg. Chem.*, **5**, 1709 (1966).
(12) D. P. Tate, *J. Polym. Sci. Polym. Symp.*, **No. 48**, 33 (1974).
(13) G. Allen, C. J. Lewis, and S. M. Todd, *Polymer*, **11**, 44 (1970).
(14) D. P. Tate and T. A. Antkowiak, *Kirk-Othmer Encycl. Chem. Technol.*, **10**, 936 (1980).
(15) H. R. Allcock, R. A. Arcus, and E. G. Stroh, *Macromolecules*, **13**, 919 (1980).
(16) N. S. Schneider, C. R. Desper, and J. J. Beres, in "Liquid Crystalline Order in Polymers", A. Blumstein, Ed., Academic Press, New York, 1978, Chapter 9, p 299.
(17) M. Kojima and J. H. Magill, *Polym. Commun.*, **24**, 329 (1983).
(18) D. W. Carlson, E. O'Rourke, J. K. Valitis, and A. G. Altenau, *J. Polym. Sci., Polym. Chem. Ed.*, **14**, 1379 (1976).
(19) M. Zeldin, W. H. Ho, and E. M. Pearce, *Macromolecules*, **13**, 1163 (1980).
(20) N. S. Schneider, C. R. Desper, and R. E. Singler, *J. Appl. Polym. Sci.*, **12**, 566 (1976).
(21) B. Chu and E. Gulari, *Macromolecules*, **12**, 445 (1979).
(22) D. P. Tate, private communication, 1983.
(23) S. V. Peddada and J. H. Magill, ONR Interim Technical Report No. 8, NR 356-644, Sept 30, 1982.
(24) D. Sinclair, U.S. Patent 4 242 316, Dec 30, 1980.
(25) H. Hiroaka, W. Lee, L. W. Welsh, Jr., and R. W. Allen, *Macromolecules*, **12**, 753 (1979).
(26) K. H. Gardner, J. H. Magill, and E. D. T. Atkins, *Polymer*, **19**, 370 (1978).
(27) J. E. Mark and C. U. Yu, *J. Polymer Sci., Polym. Phys. Ed.*, **15**, 371 (1977).
(28) H. R. Allcock, R. W. Allen, and J. J. Meister, *Macromolecules*, **9**, 950 (1976).
(29) M. M. Coleman, J. Zarian, and P. C. Painter, *Appl. Spectrosc.*, **36** (3), 277 (1982).
(30) M. Kojima, W. Kluge, and J. H. Magill, *Macromolecules*, **17**, 1421 (1984).
(31) I. C. Choy and J. H. Magill, *J. Appl. Polym. Sci.*, **19**, 2495 (1981).
(32) P. K. Ho and M. C. Williams, *Poly. Eng. Sci.*, **21**, 233 (1981).
(33) W. M. Reichert, F. E. Filsko, and S. A. Barenberg, *J. Biomed. Mater. Res.*, **16**, 301 (1982).
(34) C. E. Carrahar, Jr., 179th National Meeting of the American Chemical Society, Houston, TX, March 1980.
(35) K. A. Reynard, R. W. Sicka, A. H. Gerber, and S. H. Rose, *J. Soc. Eng., London*, **10**, 682 (1974).
(36) A. K. Chattopadhyay, R. L. Hinricks, and S. H. Rose, *J. Coat. Technol.*, **51**, 87 (1979).
(37) W. M. Widenor, Firemen Program Review, NASS Ames Research Center, Moffett Field, CA, Apr 13–14, 1978.
(38) E. J. Quinn and R. L. Dieck, *J. Fire Flammability*, **7**, 358 (1975); **8**, 412 (1976).
(39) S. V. Peddada and J. H. Magill, *Macromolecules*, **16**, 1258 (1983).
(40) P. J. Lieu, J. H. Magill, and Y. C. Alarie, *J. Fire Combust. Toxicol.*, **7**, 143 (1980); **8**, 242 (1981).
(41) D. J. Plazek, *Methods Exp. Phys.*, **16**, 52 (1980).
(42) D. J. Plazek, *J. Polymer Sci., A2*, **6**, 621 (1968).
(43) J. D. Ferry, "Viscoelastic Properties of Polymers", 3rd ed., Wiley, New York, 1980, pp 38–39.
(44) M. Kojima and J. H. Magill, *Polymer*, submitted.
(45) C. R. Desper, R. E. Singler, and N. S. Schneider, IUPAC Symposium, July 12–16, 1982, Amherst, MA, p 682.
(46) B. Wunderlich and J. Grebowicz, *Adv. Polym. Sci.*, to be published.
(47) G. W. Smith, *Adv. Liq. Cryst.*, **1** (1975).
(48) G. W. Gray, "Molecular Structure and the Properties of Liquid Crystals", Academic Press, New York, 1962.
(49) M. N. Alexander, C. R. Desper, P. L. Sagalyn, and N. S. Schneider, *Macromolecules*, **10**, 721 (1977).
(50) M. Kojima and J. H. Magill, presented at the American Physical Society (DHPP) Meeting, Detroit, Mar 26–30, 1984.
(51) J. H. Magill and D. J. Plazek, *J. Chem. Phys.*, **46**, 3757 (1967).
(52) M. J. Shankar Narayanan and J. H. Magill, unpublished work.
(53) It is important to state here that linearity checks of the viscoelastic response in creep were made from time to time during these runs.
(54) Flow is defined as permanent deformation which accumulates linearly in time under constant stress even at infinitesimally small values of the stress.